Serotonin regulates mitochondrial biogenesis and function in rodent cortical neurons via the 5-HT₂A receptor and SIRT1–PGC-1α axis

Sashaina E. Fanibunda[a,b], Sukrita Deb[a], Babukrishna Maniyadath[a], Praachi Tiwari[a], Utkarsha Ghai[a], Samir Gupta[a], Dwight Figueiredo[a], Noelia Weisstaub[c], Jay A. Gingrich[d], Ashok D. B. Vaidya[b], Ullas Kolthur-Seetharam[a,1,2], and Vidita A. Vaidya[a,1,2]

[a]Department of Biological Sciences, Tata Institute of Fundamental Research, Mumbai 400005, India; [b]Medical Research Centre, Kasturba Health Society, Mumbai 400056, India; [c]Institute of Cognitive and Translational Neuroscience (INCyT), CONICET–Favaloro University–Institute of Cognitive Neurology (INECO), C1078AAI Buenos Aires, Argentina; and [d]Department of Psychiatry, Columbia University, New York, NY 10032

Mitochondria in neurons, in addition to their primary role in bioenergetics, also contribute to specialized functions, including regulation of synaptic transmission, Ca^{2+} homeostasis, neuronal excitability, and stress adaptation. However, the factors that influence mitochondrial biogenesis and function in neurons remain poorly elucidated. Here, we identify an important role for serotonin (5-HT) as a regulator of mitochondrial biogenesis and function in rodent cortical neurons, via a 5-HT₂A receptor-mediated recruitment of the SIRT1–PGC-1α axis, which is relevant to the neuroprotective action of 5-HT. We found that 5-HT increased mitochondrial biogenesis, reflected through enhanced mtDNA levels, mitotracker staining, and expression of mitochondrial components. This resulted in higher mitochondrial respiratory capacity, oxidative phosphorylation (OXPHOS) efficiency, and a consequential increase in cellular ATP levels. Mechanistically, the effects of 5-HT were mediated via the 5-HT₂A receptor and master modulators of mitochondrial biogenesis, SIRT1 and PGC-1α. SIRT1 was required to mediate the effects of 5-HT on mitochondrial biogenesis and function in cortical neurons. In vivo studies revealed that 5-HT₂A receptor stimulation increased cortical mtDNA and ATP levels in a SIRT1-dependent manner. Direct infusion of 5-HT into the neocortex and chemogenetic activation of 5-HT neurons also resulted in enhanced mitochondrial biogenesis and function in vivo. In cortical neurons, 5-HT enhanced expression of antioxidant enzymes, decreased cellular reactive oxygen species, and exhibited neuroprotection against excitotoxic and oxidative stress, an effect that required SIRT1. These findings identify 5-HT as an upstream regulator of mitochondrial biogenesis and function in cortical neurons and implicate the mitochondrial effects of 5-HT in its neuroprotective action.

5-HT | 5-HT2A receptor | mitochondria | sirtuin 1 | neuronal survival

Serotonin (5-HT), a phylogenetically ancient molecule, in addition to its multifaceted neurotransmitter function, has been hypothesized to retain "prenervous" roles, including trophic and morphogen-like actions (1, 2). Through an influence on neurite outgrowth, synaptogenesis, and synaptic plasticity, 5-HT exerts potent effects on neuronal plasticity in the developing and mature nervous system (1, 3). It also evokes trophic factor-like effects on cell proliferation, survival, and differentiation (2).

Mitochondria are highly dynamic organelles that are vital not only for their bioenergetic role and their influence on cell survival, but also subserve specialized functions of regulating excitability, synaptic transmission, buffering Ca^{2+} homeostasis, and modulating structural and functional synaptic plasticity in the context of neurons (4). Mitochondrial biogenesis and function in neurons are hypothesized to promote cell viability and mediate effective stress adaptation (5). The vital importance of mitochondria in the context of neurons (4, 5) underscores the importance of studying upstream pathways that drive mitochondrial biogenesis and function in neurons.

Mitochondrial biogenesis and function require the coordinated transcription of nuclear- and mitochondrial-encoded genes and are mediated via transcriptional regulators that respond to extracellular and mitochondrial cues (6, 7). Several reports indicate that the NAD^+-dependent deacetylase SIRT1 and peroxisome proliferator-activated receptor gamma coactivator 1-alpha (PGC-1α) serve as master regulators of mitochondrial biogenesis and function by controlling gene expression (6, 8). While SIRT1 and PGC-1α are implicated in neuronal bioenergetics and survival (8), the upstream cues that recruit the SIRT1–PGC-1α axis in neurons remain relatively unexplored. It has been reported that 5-HT increases axonal transport of mitochondria in hippocampal neurons (9), and an influence of 5-HT₁F receptor activation on mitochondrial biogenesis in dopaminergic neurons has been recently demonstrated (10).

We hypothesized that 5-HT may exert a putative trophic-like action by serving as an upstream regulator of mitochondrial biogenesis in neurons. To test this hypothesis, we used both in vitro cortical neuronal cultures and in vivo studies, employing pharmacological and genetic perturbation strategies, and identified a hitherto-unknown role of 5-HT as a major regulator of mitochondrial biogenesis and function in cortical neurons, via a

Significance

Neuronal mitochondria are crucial organelles that regulate bioenergetics and also modulate survival and function under environmental challenges. Here, we show that the neurotransmitter serotonin (5-HT) plays an important role in the making of new mitochondria (mitochondrial biogenesis) in cortical neurons, through the 5-HT₂A receptor and via master regulators of mitochondrial biogenesis, SIRT1 and PGC-1α. Mitochondrial function is also enhanced by 5-HT, increasing cellular respiration and ATP, the energy currency of the cell. We found 5-HT reduces cellular reactive oxygen species and exerts potent neuroprotective action in neurons challenged with stress, an effect that requires SIRT1. These findings highlight a role for the mitochondrial effects of 5-HT in the facilitation of stress adaptation and identify drug targets to ameliorate mitochondrial dysfunction in neurons.

5-HT$_{2A}$ receptor-mediated recruitment of the SIRT1–PGC-1α axis. The effects of 5-HT on mitochondrial biogenesis and function play a central role in the ability of 5-HT to promote neuronal survival in response to excitotoxic or oxidative insults. Our results highlight an important function of 5-HT in the modulation of mitochondrial biogenesis and function in neurons, which facilitates stress adaptation and survival.

Results

Mitochondrial Biogenesis and Function Are Regulated by 5-HT. We examined the influence of the monoamine 5-HT on mitochondrial mass in cortical neurons in vitro by assessing mitotracker staining, which revealed a significant increase in staining intensity in 5-HT–treated neurons (Fig. 1 *A–C*). Immunofluorescence intensity measurements for the mitochondrial voltage-dependent anion channel (VDAC) demonstrated significantly increased levels following exposure to 5-HT (Fig. 1 *D* and *E*). Elevated levels of the mitochondrial outer (VDAC) and inner (cytochrome C; Cyt C) membrane marker proteins also corroborated the increased mitochondrial mass noted following 5-HT treatment (Fig. 1 *F–H* and *SI Appendix*, Fig. S1 *A–C*). Mitochondrial biogenesis is modulated by the expression of nuclear- and mitochondrial-encoded genes, which is orchestrated by master regulators such as PGC-1α, nuclear respiratory factor (*Nrf1*), and transcription factor A mitochondrial (TFAM) that

mediate mtDNA replication. PGC-1α (Fig. 1*G* and *SI Appendix*, Fig. S1*D*) and TFAM (Fig. 1*H* and *SI Appendix*, Fig. S1*E*) protein levels were significantly elevated following 5-HT exposure. The 5-HT treatment also evoked a dose-dependent up-regulation of *Ppargc1a* (Fig. 1*I*), *Tfam* (Fig. 1*J*), and *Nrf1* (*SI Appendix*, Fig. S1*F*) transcripts. A dose-dependent increase in mtDNA content (Fig. 1*K*) confirmed enhanced mitochondrial biogenesis in response to 5-HT treatment. Time-course analysis (*SI Appendix*, Fig. S1 *G–Q*) indicated a significant increase in PGC-1α expression, at the mRNA (*SI Appendix*, Fig. S1 *G–J*) and protein (*SI Appendix*, Fig. S1*K*) levels, with transcriptional changes noted as early as 4 h after 5-HT treatment. We also observed increased expression of *Ppargc1a*, *Tfam*, *Nrf1*, and *Cycs* at the 6-h time point (*SI Appendix*, Fig. S1*H*). The time-course analysis indicates two phases of transcriptional regulation of mitochondrial biogenesis regulatory genes, with the first phase noted as early as 4–6 h, with a return to baseline and a second phase observed at 48 h (*Ppargc1a*, *SI Appendix*, Fig. S1 *I* and *J*; and *Nrf1*, *SI Appendix*, Fig. S1 *L* and *N*) or 72 h (*Tfam*; *SI Appendix*, Fig. S1 *L* and *M*), following onset of 5-HT treatment. This preceded the 5-HT–evoked increase in mtDNA (*SI Appendix*, Fig. S1 *O* and *P*), highlighting the induction of a transcriptional program that may mediate 5-HT–dependent mitochondrial biogenesis.
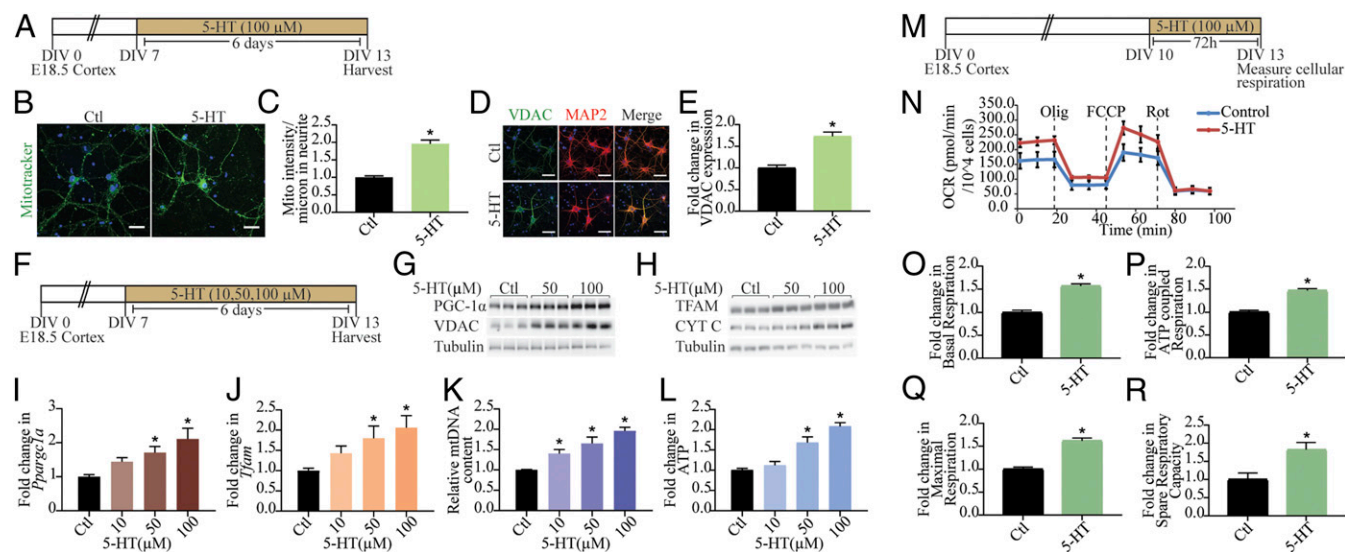
Fig. 1. Mitochondrial biogenesis and function are regulated by 5-HT. (*A*) Shown is a schematic depicting the treatment paradigm with 5-HT (100 μM) in cultured cortical neurons, commencing at day in vitro (DIV) 7 until DIV 13. (*B*) Shown are representative confocal images for Mitotracker Green staining in control (Ctl) and 5-HT–treated (100 μM) neurons, with nuclei counterstained with Hoechst 33342 (blue). (Scale bars: 30 μm; magnification: 60×.) (*C*) Quantitative analysis of fluorescence intensity represented as mitotracker (mito) intensity per micrometer of neurite ± SEM (*n* = 56 neurons in control, *n* = 59 neurons for 5-HT treatment, mean values ± SEM compiled across *N* = 3). **P* < 0.05 (compared with control, unpaired Student's *t* test). (*D*) Shown are representative immunofluorescence images for VDAC (green), neuronal marker MAP2 protein (red), and merge (yellow) from control and 5-HT–treated (100 μM) neurons. Nuclei are counterstained with Hoechst 33342 (blue). (Scale bars: 50 μm; magnification: 60×.) (*E*) Quantitative analyses for VDAC fluorescence intensity are represented as fold change in VDAC expression compared with control ± SEM (*n* = 86 neurons in control, *n* = 78 neurons for 5-HT treatment, mean values ± SEM compiled across *N* = 3). **P* < 0.05 (compared with control, unpaired Student's *t* test). (*F*) Shown is a schematic depicting treatment of neurons with increasing doses of 5-HT (10, 50, and 100 μM). (*G* and *H*) Shown are representative immunoblots for PGC-1α, VDAC, and tubulin as the loading control (*G*) and TFAM, Cyt C, and tubulin as loading control (*H*) in neurons treated with increasing doses of 5-HT (50 and 100 μM). (*I* and *J*) Quantitative PCR (qPCR) analysis for mRNA expression of key regulators of mitochondrial biogenesis *Ppargc1a* (*I*) and *Tfam* (*J*) are represented as fold change of control ± SEM (representative results from *n* = 4 per treatment group/*N* = 3). **P* < 0.05 (compared with control, one-way ANOVA, Tukey's post hoc test). (*K*) qPCR analyses for mtDNA levels are represented as relative mtDNA content ± SEM (representative results from *n* = 4–6 per treatment group/*N* = 3). **P* < 0.05 (compared with control, one-way ANOVA, Tukey's post hoc test). (*L*) Quantitation of ATP levels expressed as fold change of control ± SEM (representative results from *n* = 4 per treatment group/*N* = 4). **P* < 0.05 (compared with control, one-way ANOVA, Tukey's post hoc test). (*M*) Shown is a schematic for the treatment paradigm with 5-HT (100 μM) (DIV 10–13) for Seahorse analysis of cellular respiration. (*N*) Shown is a representative Seahorse plot for control and 5-HT–treated cortical neurons, with measurements of OCR (normalized to cell numbers per well), baseline, and following treatment of cells with oligomycin (Olig), FCCP, and rotenone (Rot), as indicated. (*O–R*) Quantitative analysis of the effects of 5-HT on basal respiration (*O*), ATP-coupled respiration (*P*), maximal respiration (*Q*), and spare respiratory capacity (*R*) expressed as fold change of control ± SEM (compiled results from *n* = 5 per treatment group/*N* = 3). **P* < 0.05 (compared with control, unpaired Student's *t* test).

We next sought to determine if 5-HT altered bioenergetics in cortical neurons and observed that 5-HT treatment resulted in enhanced cellular ATP levels in a dose-dependent (Fig. 1L) and time-dependent (*SI Appendix*, Fig. S1 *O* and *Q*) manner. These effects appeared to be selective to 5-HT, as neither norepinephrine (NE) nor dopamine (DA) influenced mtDNA content (*SI Appendix*, Fig. S1 *R* and *S*) or ATP (*SI Appendix*, Fig. S1 *R* and *T*) levels in cortical neurons. On assaying for oxidative phosphorylation (OXPHOS) and electron transport chain efficiency, by measuring oxygen-consumption rate (OCR) (Fig. 1 *M* and *N*), we found a robust increase in basal OCR (~50%) (Fig. 1O) in 5-HT–treated cortical neurons, accompanied by an increase in ATP-coupled respiration (Fig. 1P). Treatment with the mitochondrial uncoupler FCCP revealed a higher maximal respiration (Fig. 1Q) in 5-HT–treated cortical neurons, concomitant with an increase in spare respiratory capacity (Fig. 1R), compared with controls. These findings indicate that, in addition to modulating mitochondrial biogenesis, 5-HT also exerts an important regulatory control on OXPHOS and leads to enhanced mitochondrial function in cortical neurons.

Effects of 5-HT on Mitochondrial Biogenesis and Function Are Mediated via the 5-HT$_{2A}$ Receptor.

We carried out pharmacological and genetic perturbation studies to determine the contribution of specific 5-HT receptors to the effects of 5-HT on mitochondria. Cortical neurons express several 5-HT receptors, among which the 5-HT$_{2A}$ and 5-HT$_{1A}$ receptors are expressed at high levels (*SI Appendix*, Fig. S2 *A* and *B*). The 5-HT$_{2A}$ receptor antagonist MDL100,907 completely inhibited the 5-HT–evoked increase in mtDNA content (Fig. 2 *A* and *B*) and *Ppargc1a* expression. (Fig. 2C). Furthermore, the 5-HT–mediated induction of ATP levels was also prevented by treatment with MDL100,907 (Fig. 2D). A role for 5-HT$_{2A}$ receptors in regulation of mitochondrial biogenesis and energetics was further supported by evidence of a dose-dependent increase in mtDNA (Fig. 2 *E* and *F*), *Ppargc1a* expression (Fig. 2G), and ATP levels (Fig. 2H) following treatment with the 5-HT$_{2A}$ receptor agonist 2,5-dimethoxy-4-iodoamphetamine (DOI). In addition to significant increases in mitochondrial biogenesis and function evoked by DOI, a 5-HT$_{2A}$ receptor agonist with hallucinogenic effects, we also noted that a nonhallucinogenic 5-HT$_{2A}$ receptor agonist lisuride (*SI Appendix*, Fig. S2C) could also increase mtDNA (*SI Appendix*, Fig. S2D), *Ppargc1a* expression (*SI Appendix*, Fig. S2E), and ATP levels (*SI Appendix*, Fig. S2F). Treatment with the 5-HT$_{1A}$ receptor antagonist WAY100,635 did not alter the 5-HT–mediated increase in mtDNA (*SI Appendix*, Fig. S2 *G* and *H*) and ATP (*SI Appendix*, Fig. S2I) levels. To address whether 5-HT$_{2A}$ receptor stimulation with DOI influences mitochondrial respiration, we measured OCR (Fig. 2 *I* and *J*). Cortical neurons treated with DOI exhibited significant increases in both basal OCR (Fig. 2K) and ATP-coupled respiration (Fig. 2L), accompanied by enhanced maximal respiration (Fig. 2M) and spare respiratory capacity (Fig. 2N). Importantly, the effects of 5-HT on mitochondrial biogenesis and OXPHOS were recapitulated by treatment with the 5-HT$_{2A}$ receptor agonist DOI.

We further characterized the contribution of the 5-HT$_{2A}$ receptor, using cortical neurons derived from 5-HT$_{2A}$ receptor knockouts (5-HT$_{2A}$$^{-/-}$), compared with wild-type (WT) and 5-HT$_{2A}$$^{-/-Res}$ cortical cultures (Fig. 2 *O* and *P* and *SI Appendix*, Fig. S2 *J* and *K*). The 5-HT–mediated increase in mtDNA content (Fig. 2Q) and *Ppargc1a* expression (Fig. 2R) was completely abrogated in 5-HT$_{2A}$$^{-/-}$ cortical neurons and was restored in 5-HT$_{2A}$$^{-/-Res}$ cells, wherein a viral-based gene delivery of rAAV8–CaMKIIα–GFP–Cre was utilized to rescue *Htr2a* expression in cortical neurons (*SI Appendix*, Fig. S2 *J* and *K*). Furthermore, the induction of ATP levels noted following 5-HT treatment to WT neurons was absent in cortical cultures derived from 5-HT$_{2A}$ receptor knockouts and was reinstated on rescue of 5-HT$_{2A}$ receptor expression (Fig. 2S). Together, these results illustrate that the 5-HT$_{2A}$ receptor is necessary for the effects of 5-HT on mitochondrial biogenesis and energetics.

Having identified the 5-HT$_{2A}$ receptor as a key determinant of the effects of 5-HT on mitochondria, we next sought to delineate the contribution of specific downstream signaling pathways. Cortical neurons were incubated with 5-HT in the presence of U73122, U0126, and LY294002, specific inhibitors for the phospholipase C (PLC), MEK, and phosphatidylinositol 3-kinase (PI3K) signaling pathways, respectively (Fig. 2 *T* and *U* and *SI Appendix*, Fig. S2 *L–P*). The 5-HT treatment resulted in robust activation of phospho-PLC (pPLC) (Fig. 2U and *SI Appendix*, Fig. S2M) and phospho-ERK (pERK) (Fig. 2U and *SI Appendix*, Fig. S2N), but not of phospho-Akt (pAkt) (*SI Appendix*, Fig. S2 *O* and *P*), which lies downstream of PI3K. The 5-HT–mediated increase in mtDNA content (Fig. 2V) and *Ppargc1a* expression (Fig. 2W) were partially blocked by both PLC and MEK inhibitors, but not by PI3K inhibition (Fig. 2 *V* and *W*). These findings implicate signaling via the PLC and MAPK/ERK cascades in the effects of 5-HT on mitochondrial biogenesis. Collectively, these results indicate that 5-HT via the 5-HT$_{2A}$ receptor and the PLC and MAPK signaling pathways modulate mitochondrial biogenesis.

Sirt1 Is Required for the Effects of 5-HT on Mitochondrial Biogenesis and Function.

SIRT1, a NAD$^+$-dependent deacetylase, is well established to induce mitochondrial biogenesis and functions by its ability to regulate transcription involving PGC-1α (6). In cortical neurons, we observed an up-regulation of *Sirt1* mRNA as early as 4 h (Fig. 3 *A* and *B*), with a return to baseline noted at 8 h after commencement of 5-HT treatment. We also noted a sustained up-regulation of *Sirt1* mRNA observed at 48 h onward (Fig. 3C), with a commensurate increase in SIRT1 protein levels at 48 h (Fig. 3 *D* and *E*). The transcriptional up-regulation of *Sirt1* by 5-HT was blocked by coadministration of the 5-HT$_{2A}$ receptor antagonist MDL100,907 (*SI Appendix*, Fig. S3 *A* and *B*) and mimicked by the 5-HT$_{2A}$ receptor agonist DOI (*SI Appendix*, Fig. S3 *C* and *D*). We investigated the possible involvement of SIRT1 in the actions of 5-HT on mitochondria by treating cortical neurons with 5-HT in the presence of EX-527, a selective chemical inhibitor of SIRT1 activity (Fig. 3F). EX-527 treatment abrogated the 5-HT–induced increase in mtDNA content (Fig. 3G) and mitochondrial mass in neurites (Fig. 3 *H* and *I*). Furthermore, coadministration of EX-527 with 5-HT failed to exhibit the 5-HT–evoked up-regulation of *Ppargc1a* (Fig. 3J), *Tfam* (Fig. 3K), *Nrf1* (*SI Appendix*, Fig. S3 *E* and *F*), and *Cycs* (*SI Appendix*, Fig. S3G). We then examined the consequences of SIRT1 inhibition and found that the 5-HT–mediated increase in ATP levels was abrogated in the presence of EX-527 (Fig. 3L). To further ascertain the contribution of SIRT1 to the regulation of ATP levels by 5-HT, we used cortical neurons derived from SIRT1 conditional knockout (Sirt1cKO) embryos (Fig. 3M). Treatment with 5-HT failed to induce cellular ATP levels in cortical neurons from Sirt1cKO, compared with WT controls, thus demonstrating an essential role for SIRT1 in mediating the effects of 5-HT (Fig. 3N). We next examined the influence of 5-HT on cortical neurons derived from SirT1$^{lox/lox}$ embryos and in vitro transduced with adeno-associated virus (AAV) Cre– or AAV Cre+ to yield control (SirT1$^{lox/lox}$) or SIRT1 loss-of-function (SirT1$^{co/co}$) neurons, respectively (Fig. 3O and *SI Appendix*, Fig. S3H). Treatment with 5-HT did not alter gene expression of *Ppargc1a* (Fig. 3P), *Tfam* (Fig. 3Q), *Nrf1* (*SI Appendix*, Fig. S3I), or *Cycs* (*SI Appendix*, Fig. S3J) in the absence of SIRT1 (SirT1$^{co/co}$), in contrast to the robust up-regulation noted in control SirT1$^{lox/lox}$ cortical neurons. Together, our pharmacological and genetic perturbation studies illustrate the role of SIRT1 in mediating the mitochondrial effects of 5-HT.

Neuroprotective Effects of 5-HT Against Excitotoxic and Oxidative Stress Are Mediated via the 5-HT$_{2A}$ Receptor and SIRT1.

Given that 5-HT exerts robust effects on mitochondria, which are major
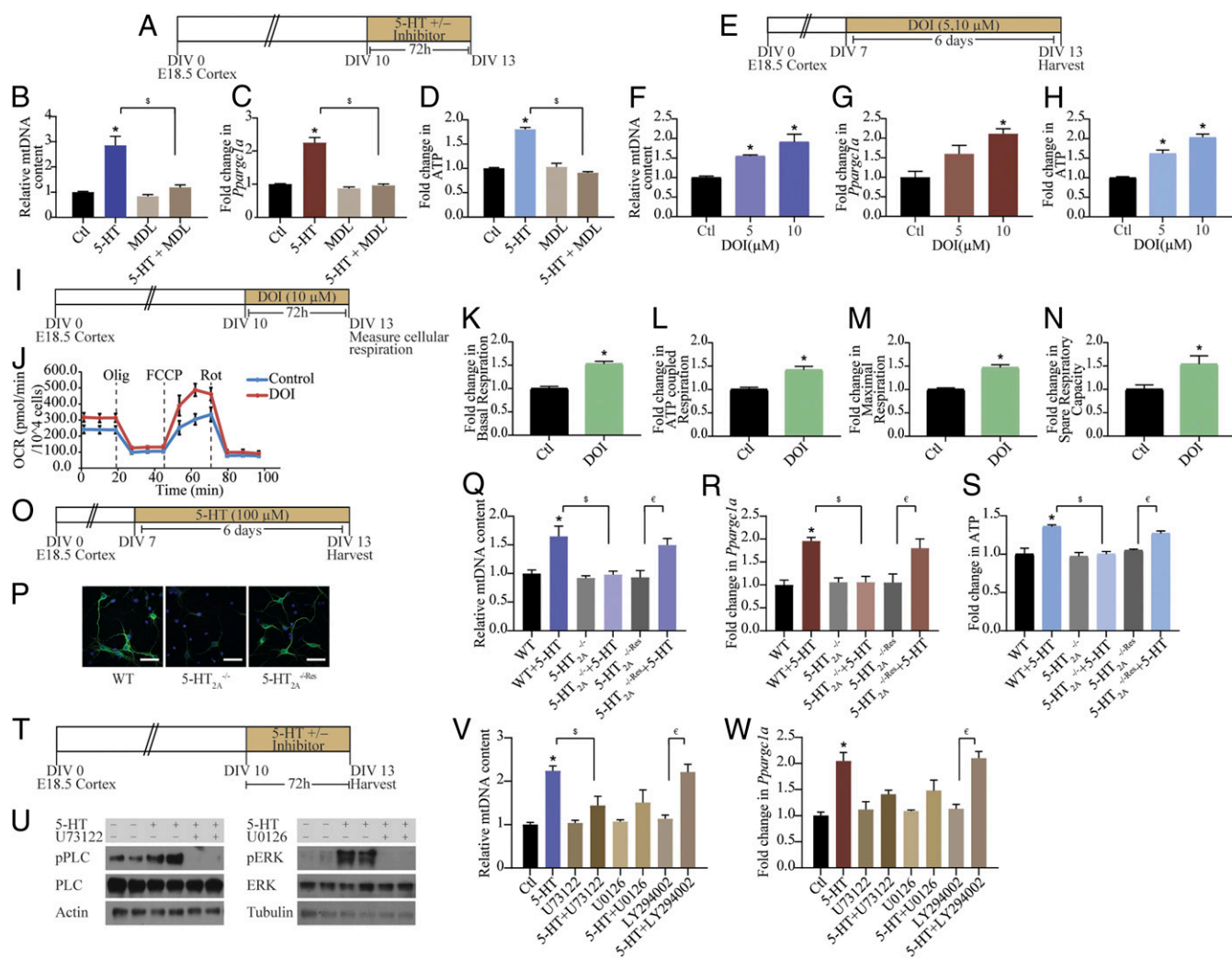
Fig. 2. Mitochondrial effects of 5-HT are mediated via the 5-HT$_{2A}$ receptor. (*A*) Shown is a schematic depicting the treatment paradigm for cortical neuron cultures with 5-HT (100 μM), MDL100,907 (10 μM), and 5-HT+MDL100,907 for 72 h commencing on DIV 10. (*B–D*) Quantitation of mtDNA (*B*), *Ppargc1a* mRNA (*C*), and ATP (*D*) levels in cortical neurons treated with 5-HT in the presence or absence of MDL100,907 (MDL) are represented as fold change of control (Ctl) ± SEM [representative results from $n = 4$ per treatment group/$N = 2$ (mtDNA and ATP) and $N = 3$ (*Ppargc1a* mRNA)]. *$P < 0.05$ (compared with control); $^{\$}P < 0.05$ (compared with 5-HT–treated group); two-way ANOVA, Tukey's post hoc test. (*E*) Shown is a schematic depicting the treatment paradigm for cortical neurons with increasing doses of DOI (5 and 10 μM) from DIV 7 to 13. (*F–H*) Quantitation of mtDNA (*F*), *Ppargc1a* mRNA (*G*), and ATP (*H*) levels in neurons treated with DOI are represented as fold change of control ± SEM (representative results from $n = 4$ per treatment group/$N = 2$). *$P < 0.05$ (compared with control, one-way ANOVA, Tukey's post hoc test). (*I*) Shown is a schematic depicting the treatment paradigm of cortical neurons with DOI (10 μM) for Seahorse analysis of cellular respiration starting DIV 10. (*J*) Shown is a representative Seahorse plot for control and DOI-treated cortical neurons, with measurements of OCR (normalized to cell numbers per well) at baseline and following treatment with oligomycin (Olig), FCCP, and rotenone (Rot), as indicated. (*K–N*) Bar graphs depict quantitative analysis of the effects of DOI on basal respiration (*K*), ATP-coupled respiration (*L*), maximal respiration (*M*), and spare respiratory capacity (*N*) expressed as fold change of control ± SEM (compiled results from $n = 4$ or 5 per treatment group/$N = 3$). *$P < 0.05$ (compared with control, unpaired Student's *t* test). (*O*) Shown is a schematic depicting the treatment paradigm of WT, 5-HT$_{2A}^{-/-}$, and 5-HT$_{2A}^{-/-\text{Res}}$ cortical neurons with 5-HT (100 μM). (*P*) Shown are representative images for 5-HT$_{2A}$ receptor immunofluorescence (green) from WT, 5-HT$_{2A}^{-/-}$, and 5-HT$_{2A}^{-/-\text{Res}}$ cortical neuron cultures with nuclei counterstained with Hoechst 33342 (blue). (Scale bars: 50 μm; magnification: 60×.) (*Q–S*) Graphs depict quantitative analysis for mtDNA (*Q*), *Ppargc1a* mRNA (*R*), and ATP (*S*) levels in WT, 5-HT$_{2A}^{-/-}$, and 5-HT$_{2A}^{-/-\text{Res}}$ cortical neurons treated with 5-HT, and results are represented as fold change of WT ± SEM (representative results from $n = 4$ per treatment group/$N = 2$). *$P < 0.05$ (compared with WT); $^{\$}P < 0.05$ (compared with WT+5-HT); $^{€}P < 0.05$ (compared with 5-HT$_{2A}^{-/-\text{Res}}$); two-way ANOVA, Tukey's post hoc test. (*T*) Shown is a schematic depicting the treatment paradigm of cortical neurons with 5-HT (100 μM) in the presence or absence of signaling inhibitors for PLC (U73122; 5 μM), MEK (U0126; 10 μM), and PI3K (LY294002; 10 μM). (*U*) Shown are representative immunoblots for pPLC and PLC levels in cortical neurons treated with 5-HT in the presence or absence of the PLC inhibitor U73122 and for pERK and ERK levels in cortical neurons treated with 5-HT in the presence or absence of the MEK inhibitor U0126. Actin and tubulin immunoblots serve as the loading controls. (*V* and *W*) Quantitative analysis for mtDNA (*V*) and *Ppargc1a* mRNA (*W*) levels in cortical neurons treated with 5-HT in the presence or absence of PLC, MEK, and PI3K inhibitors are represented as fold change of control ± SEM (representative results from $n = 4$ per treatment group/$N = 2$). *$P < 0.05$ (compared with control); $^{\$}P < 0.05$ (compared with 5-HT–treated group); $^{€}P < 0.05$ (compared with LY294002 group); two-way ANOVA, Tukey's post hoc test.

sites of reactive oxygen species (ROS) production and scavenging, we next examined 5-HT effects on cellular ROS levels. We assessed the influence of 5-HT both at baseline and in the context of challenge with excitotoxic (kainate) (Fig. 4 *A* and *B*) and oxidative (hydrogen peroxide; H$_2$O$_2$) stressors (Fig. 4 *A* and *B*). Fluorometric analysis of cellular ROS levels indicated a baseline reduction following 5-HT treatment (Fig. 4 *C* and *D*) compared with control cortical neurons. Furthermore, 5-HT pretreatment robustly attenuated the increased ROS levels observed following treatment with kainate (Fig. 4 *B* and *C*)
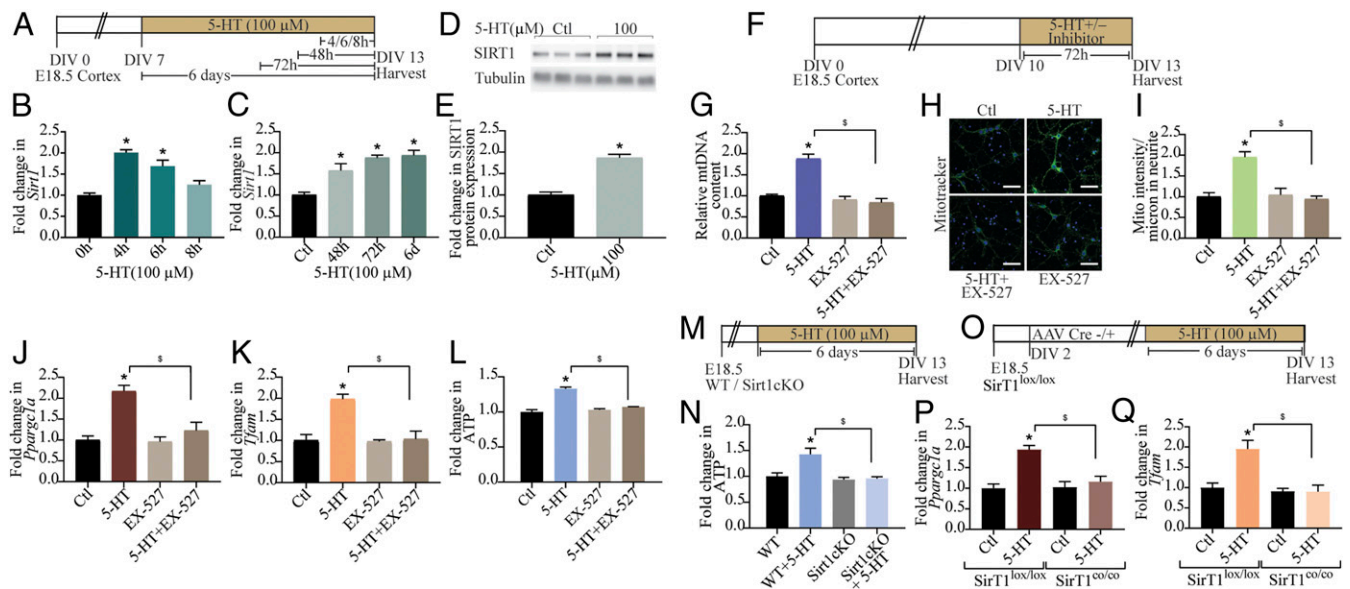
Fig. 3. SIRT1 is required for the effects of 5-HT on mitochondria. (*A*) Shown is a schematic depicting the treatment paradigm of neurons with 5-HT (100 μM) for 4, 6, 8, 48, and 72 h and 6 d and lysed synchronously at DIV 13. (*B* and *C*) qPCR analysis for *Sirt1* mRNA expression is expressed as fold change of control (Ctl) ± SEM (representative results from *n* = 4 per treatment group/*N* = 2). *$P < 0.05$ (compared with control, one-way ANOVA, Tukey's post hoc test). (*D*) Shown is a representative immunoblot for SIRT1 protein expression and the loading control tubulin from control and 5-HT–treated (100 μM) cortical neurons at 48 h. (*E*) Quantitative densitometric analysis of SIRT1 levels normalized to tubulin. Results are expressed as fold change of control ± SEM (compiled results from *n* = 6 per treatment group/*N* = 2). *$P < 0.05$ (compared with control, unpaired Student's *t* test). (*F*) Shown is a schematic depicting the treatment paradigm of neurons with 5-HT (100 μM) in the presence or absence of SIRT1 inhibitor EX-527 (10 μM) commencing on DIV 10. (*G*) Quantitation of mtDNA in 5-HT–treated cortical neurons in the presence or absence of EX-527 are represented as fold change of control ± SEM (representative results from *n* = 4 per treatment group/*N* = 3). *$P < 0.05$ (compared with control); $^{\$}P < 0.05$ (compared with 5-HT–treated group); two-way ANOVA, Tukey's post hoc test. (*H*) Shown are representative confocal images for Mitotracker Green staining in control (Ctl) and 5-HT–treated cortical neurons in the presence and absence of EX-527. (Scale bars: 50 μm; magnification: 60×.) (*I*) Quantitative analysis of fluorescence intensity represented as mitotracker (Mito) intensity per micrometer of neurite ± SEM (*n* = 39 neurons in control group, *n* = 47 neurons in 5-HT–treated group, *n* = 44 neurons in 5-HT+EX-527 group, and *n* = 33 neurons in EX-527 group, mean ± SEM compiled across *N* = 2). *$P < 0.05$ (compared with control); $^{\$}P < 0.05$ (compared with 5-HT–treated group); two-way ANOVA, Tukey's post hoc test. (*J–L*) Graphs depict quantitation of *Ppargc1a* (*J*) and *Tfam* (*K*) mRNA and cellular ATP (*L*) levels in cortical neurons treated with 5-HT in the presence or absence of EX-527 and represented as fold change of control ± SEM [representative results from *n* = 4 per treatment group/*N* = 4 (*Ppargc1a* mRNA and ATP) and *N* = 2 (*Tfam* mRNA)]. *$P < 0.05$ (compared with control); $^{\$}P < 0.05$ (compared with 5-HT–treated group); two-way ANOVA, Tukey's post hoc test. (*M*) Shown is a schematic depicting the treatment paradigm for cortical neuron cultures from Sirt1cKO and WT mice, with 5-HT (100 μM) commencing on DIV 7. (*N*) Quantitative analyses of ATP levels in WT and Sirt1cKO cortical neuron cultures following 5-HT treatment are represented as fold change of WT ± SEM (representative results from *n* = 4 per treatment group/*N* = 2). *$P < 0.05$ (compared with WT); $^{\$}P < 0.05$ (compared with WT+5-HT); two-way ANOVA, Tukey's post hoc test. (*O*) Shown is a schematic depicting the treatment paradigm for cortical neuron cultures derived from SirT1$^{lox/lox}$ embryos and then transduced in vitro on DIV 2 with rAAV8–CamKIIα–GFP (AAV-Cre−) or rAAV8–CamKIIα–GFP-Cre (AAV-Cre+) to yield control cortical neurons (SirT1$^{lox/lox}$) or cortical neurons with loss of function of SIRT1 (SirT1$^{co/co}$). SirT1$^{lox/lox}$ and SirT1$^{co/co}$ cortical neuron cultures were then treated with vehicle or 5-HT (100 μM) commencing on DIV 7. (*P* and *Q*) Graphs depict quantitation of *Ppargc1a* (*P*) and *Tfam* (*Q*) mRNA expression in SirT1$^{lox/lox}$ and SirT1$^{co/co}$ cortical neurons, in the presence or absence of 5-HT and represented as fold change of control ± SEM (representative results from *n* = 6 per treatment group/*N* = 2). *$P < 0.05$ [compared with Ctl (SirT1$^{lox/lox}$)]; $^{\$}P < 0.05$ [compared with 5-HT (SirT1$^{lox/lox}$)]; two-way ANOVA, Tukey's post hoc test.

or H_2O_2 (Fig. 4 *B* and *D*). Up-regulation of ROS scavenging enzymes superoxide dismutase 2 (*Sod2*) and catalase (*Cat*), which are known to be regulated by SIRT1/PGC-1α (11, 12), corroborated these findings and suggests putative mechanisms for 5-HT–mediated reduction of cellular ROS (*SI Appendix,* Fig. S4 *A–C*).

We then sought to examine potential neuroprotective effects of 5-HT in the context of kainate-mediated excitotoxicity or H_2O_2-mediated oxidative damage (Fig. 4*A*). Cell-survival assays, using the cell viability marker MTT, revealed that cortical neuronal survival was significantly reduced by kainate (Fig. 4*E*) and H_2O_2 (Fig. 4*F*) treatment and was attenuated in a dose-dependent fashion in 5-HT–pretreated cortical cultures. These neuroprotective effects of 5-HT were mimicked by pretreatment with DOI, which also enhanced cell survival to excitotoxic or oxidative insults (*SI Appendix,* Fig. S4 *D–F*). Given our results of a role for SIRT1 in the mitochondrial effects of 5-HT, we examined the contribution of SIRT1 to the neuroprotective action of 5-HT. Cortical neuronal cultures were pretreated with 5-HT in the presence/absence of the SIRT1 inhibitor EX-527, followed by exposure to increasing doses

of either kainate (Fig. 4 *G* and *H*) or H_2O_2 (Fig. 4 *G* and *I*). EX-527 prevented the 5-HT–mediated neuroprotective effects in response to challenge with escalating doses of kainate (Fig. 4*H*) and H_2O_2 (Fig. 4*I*). The neuroprotective actions of 5-HT were observed over a wide range of kainate and H_2O_2 doses, and SIRT1 inhibition prevented these effects. The enhanced cell viability noted in cortical neurons pretreated with the 5-HT$_{2A}$ receptor agonist DOI on kainate or H_2O_2 challenge was attenuated by EX-527 (*SI Appendix,* Fig. S4 *G–I*). These findings indicate that SIRT1 plays an important role in contributing to the neuroprotective effects of 5-HT and the 5-HT$_{2A}$ receptor agonist DOI in the context of excitotoxic and oxidative stress. This was further confirmed via evidence from Sirt1cKO cortical cultures, which, unlike WT cortical neurons, failed to exhibit the improved cell viability noted on 5-HT pretreatment before kainate-mediated (Fig. 4 *J* and *K*) or H_2O_2-mediated (Fig. 4 *J* and *L*) challenge. Together, these results indicate that 5-HT, via the 5-HT$_{2A}$ receptor and the sirtuin SIRT1, exerts robust neuroprotective effects against excitotoxic and oxidative cell death and damage.
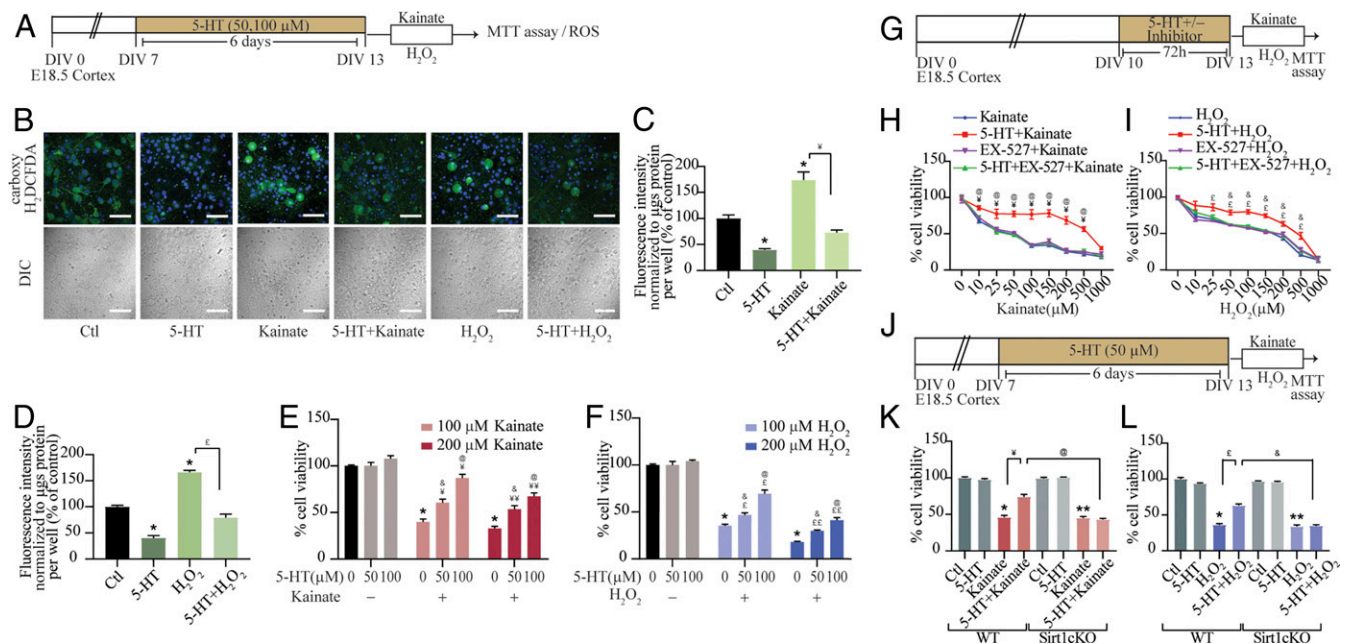
Fig. 4. Neuroprotective effects of 5-HT against excitotoxic and oxidative stress are mediated via SIRT1. (A) Shown is a schematic depicting the treatment paradigm of neurons with 5-HT (50 or 100 µM) pretreatment commencing on DIV 7 followed by exposure to the excitotoxic insult of kainate (100 and 200 µM) or oxidative stress through H_2O_2 (100 and 200 µM) on DIV 13, and analysis of cellular ROS or cell survival via the MTT assay. (B) Shown are representative confocal images of carboxy-H_2DCFDA staining (green) to measure cellular ROS in neurons treated with 5-HT (100 µM), kainate (100 µM), H_2O_2 (200 µM), 5-HT+kainate, or 5-HT+H_2O_2. Nuclei are counterstained with Hoechst 33342 (blue). Shown are the differential interference contrast (DIC) images of cortical neurons across treatment conditions. (Scale bars: 50 µm; magnification: 60×.) (C and D) Fluorometric quantitation of staining intensity of cellular ROS (carboxy-H_2DCFDA) normalized to protein content per well and represented as percent of control ± SEM (representative results from $n = 4$ per treatment group/$N = 2$). *$P < 0.05$ (compared with control); ¥$P < 0.05$ (compared with kainate-treated group); £$P < 0.05$ (compared with H_2O_2-treated group); (two-way ANOVA, Tukey's post hoc test). (E and F) Graphs depict cell viability assessed by the MTT assay in cortical neurons challenged with kainate (100 or 200 µM) or H_2O_2 (100 or 200 µM) with or without pretreatment with 5-HT (50 or 100 µM). Results are expressed as percent of control cell viability ± SEM (representative results from $n = 3$ per treatment group/$N = 2$). *$P < 0.05$ (compared with control); ¥$P < 0.05$ (compared with 100 µM kainate-treated group); ¥¥$P < 0.05$ (compared with 200 µM kainate-treated group); £$P < 0.05$ (compared with 100 µM H_2O_2-treated group); ££$P < 0.05$ (compared with 200 µM H_2O_2-treated group); &$P < 0.05$ (compared with 50 µM 5-HT–treated group); @$P < 0.05$ (compared with 100 µM 5-HT–treated group); two-way ANOVA, Tukey's post hoc test. (G) Shown is a schematic depicting the treatment paradigm of neurons with 5-HT (100 µM) in the presence or absence of the SIRT1 inhibitor EX-527 (10 µM), followed by challenge with increasing doses of kainate or H_2O_2 (0–1,000 µM) and analysis of cell viability using the MTT assay. (H) Shown is a line graph for cell viability of cortical neurons in response to increasing doses of kainate (0–1,000 µM) with treatment groups of kainate (blue), 5-HT+kainate (red), EX-527+kainate (purple), and 5-HT+EX-527+kainate (green), expressed as percent of control cell viability ± SEM (representative results from $n = 3$ per treatment group/$N = 2$). ¥$P < 0.05$ (compared with kainate-treated group); @$P < 0.05$ (compared with 5-HT+EX-527+kainate-treated group); three-way ANOVA, Tukey's post hoc test. (I) Shown is a line graph for cell viability of cortical neurons in response to increasing doses of H_2O_2 (0–1,000 µM) with treatment groups of H_2O_2 (blue), 5-HT+H_2O_2 (red), EX-527+H_2O_2 (purple), and 5-HT+EX-527+H_2O_2 (green), expressed as percent of control cell viability ± SEM (representative results from $n = 3$ per treatment group/$N = 2$). £$P < 0.05$ (compared with H_2O_2-treated group); &$P < 0.05$ (compared with 5-HT+EX-527+H_2O_2-treated group); three-way ANOVA, Tukey's post hoc test. (J) Shown is a schematic depicting the treatment paradigm of cortical neuron cultures derived from WT and Sirt1cKO embryos, with 5-HT (50 µM) treatment commencing on DIV 7, followed by a challenge with kainate (100 µM) or H_2O_2 (200 µM) on DIV 13 and analysis of cell viability. (K and L) Graph depicts cell viability of WT, WT+5-HT, Sirt1cKO, and Sirt1cKO+5-HT cortical neurons left untreated (Ctl) or challenged with kainate (K) or H_2O_2 (L) and expressed as percent of WT-Ctl cell viability ± SEM (representative results from $n = 3$ per treatment group/$N = 2$). *$P < 0.05$ (compared with WT-Ctl); **$P < 0.05$ (compared with Sirt1cKO-Ctl); ¥$P < 0.05$ (compared with WT+kainate); @$P < 0.05$ (compared with WT+5-HT+kainate); £$P < 0.05$ (compared with WT+H_2O_2); &$P < 0.05$ (compared with WT+5-HT+H_2O_2); three-way ANOVA, Tukey's post hoc test.

In Vivo Regulation of Cortical Mitochondrial DNA Content, Gene and Protein Expression, Mitochondrial OCR, and ATP by 5-HT.

Given that we noted robust effects of 5-HT, via the 5-HT$_{2A}$ receptor, on mitochondrial biogenesis and function in cortical neurons in vitro, we next sought to examine whether DOI-mediated stimulation of the 5-HT$_{2A}$ receptor led to regulation of mitochondrial biogenesis, gene/protein expression, and cellular ATP levels in vivo (Fig. 5A). Subchronic (72 h) treatment with DOI resulted in a significant increase in mtDNA content (Fig. 5B); gene expression of *Ppargc1a*, *Sirt1*, *Nrf1*, *Tfam*, and *Cycs* (Fig. 5C) in the rat neocortex; and enhanced cortical protein levels of SIRT1, TFAM, Cyt C, ATP5A, and VDAC (Fig. 5D and *SI Appendix*, Fig. S5 A–F). These transcriptional changes were also observed in vivo in DOI-treated C57BL/6NCrl/Cri mice, with a rapid induction of *Ppargc1a*, *Sirt1*, and *Tfam* (*SI Appendix*, Fig. S5 H–K) at 2 h, with a return to baseline at 24 h, and a subsequent increase noted at 48 and 72 h. We also noted enhanced cortical

cellular ATP levels in DOI-treated rats compared with vehicle-treated controls (Fig. 5E). Seahorse analysis (*SI Appendix*, Fig. S5G) performed on isolated mitochondria derived from cortices of vehicle- and DOI-treated rats revealed enhanced state-2 (via complex-I/II) and state-3 (complex II-dependent) respiration (Fig. 5F) and ATP production rate (Fig. 5G) following DOI administration. As these rates were normalized to the amount of mitochondria used in the assay, it was suggestive of higher complex I and II activity and OXPHOS efficiency following 5-HT$_{2A}$ receptor stimulation. These in vivo observations recapitulated the effects of DOI on mitochondria noted in cortical neuronal cultures.

To address whether the in vivo effects of 5-HT$_{2A}$ receptor stimulation with DOI are also triggered by 5-HT, we directly delivered 5-HT (10 µM, 7 d; Fig. 5H) into the neocortex of Sprague–Dawley rats using Alzet osmotic minipumps. Intracortical infusion of 5-HT resulted in significant increases in mtDNA (Fig. 5I) and cellular ATP (Fig. 5J) levels, indicating
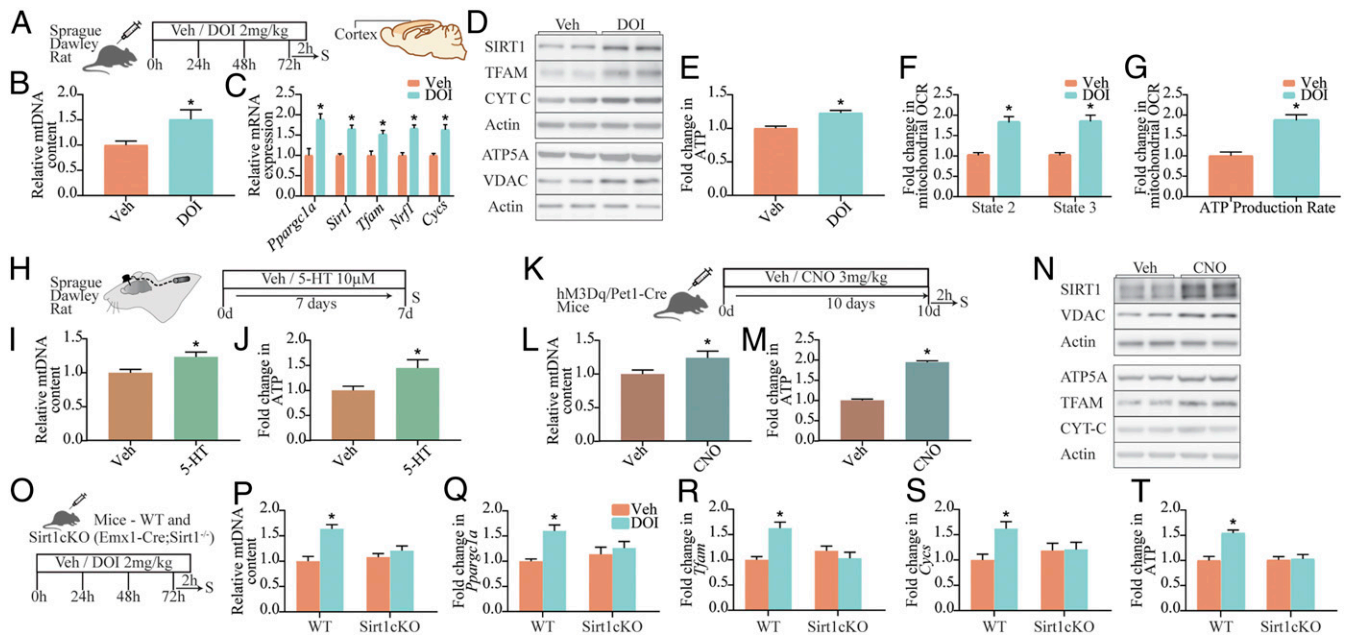
Fig. 5. In vivo regulation of cortical mitochondrial DNA content, gene and protein expression, mitochondrial OCR, and ATP by 5-HT. (*A*) Shown is a schematic of the treatment paradigm for Sprague–Dawley rats with the 5-HT$_{2A}$ receptor agonist DOI (2 mg/kg) or vehicle (Veh; saline). (*B* and *C*) Quantitation of mtDNA levels (*B*) and gene expression of *Ppargc1a*, *Sirt1*, *Tfam*, *Nrf1*, and *Cycs* (*C*) within the cortex of saline- and DOI-treated rats expressed as fold change of vehicle ± SEM (*n* = 8–11 animals per group). *$P < 0.05$ (compared with vehicle, unpaired Student's *t* test). (*D*) Shown are representative immunoblots for SIRT1, TFAM, Cyt C, ATP5A, VDAC, and actin as loading control in cortices derived from vehicle- and DOI-treated animals. (*E*) Quantitation of cellular ATP levels in cortices derived from vehicle- and DOI-treated Sprague–Dawley rats are represented as fold change of control ± SEM (*n* = 8–11 animals per group). *$P < 0.05$ (compared with vehicle, unpaired Student's *t* test). (*F* and *G*) Shown is the quantitation of state-2 (via complex-I/II) and state-3 (complex II-dependent) respiration (*F*) and ATP production rate (*G*) on isolated mitochondria (10 μg) derived from the PFC of vehicle- and DOI-treated Sprague–Dawley rats (*A*), based on Seahorse analysis, and expressed as fold change of vehicle ± SEM (*n* = 5 per treatment group/*N* = 1). *$P < 0.05$ (compared with vehicle, unpaired Student's *t* test). (*H*) Shown is a schematic of the surgical treatment paradigm to deliver 5-HT (10 μM) or vehicle via osmotic minipumps directly into the neocortex for a duration of 7 d. (*I* and *J*) Quantitation for relative mtDNA content (*I*) and cellular ATP levels (*J*) expressed as fold change of vehicle ± SEM (representative results from *n* = 6 per treatment group/*N* = 1). *$P < 0.05$ (compared with vehicle, unpaired Student's *t* test). (*K*) Shown is a representative paradigm for chemogenetic activation of serotonergic neurons using hM3Dq/Pet1–Cre bigenic mice and systemic administration of the DREADD agonist CNO (3 mg/kg, once daily for 10 d) with euthanization (S) 2 h following the final CNO administration. (*L* and *M*) Quantitation for relative mtDNA content (*L*) and cellular ATP levels (*M*) in the PFC of vehicle- and CNO-administered hM3Dq/Pet1–Cre mice is expressed as fold change of vehicle ± SEM (representative results from *n* = 6–8 per treatment group/*N* = 1). *$P < 0.05$ (compared with vehicle, unpaired Student's *t* test). (*N*) Shown are representative immunoblots for SIRT1, VDAC, ATP5A, TFAM, Cyt C, and actin as loading control in the PFC derived from vehicle- and CNO-administered hM3Dq/Pet1–Cre mice. (*O*) Shown is a schematic of the treatment paradigm for WT and Sirt1cKO mice with the 5-HT$_{2A}$ receptor agonist DOI (2 mg/kg) or vehicle. (*P*–*T*) Quantitation of mtDNA levels (*P*), mRNA expression of *Ppargc1a* (*Q*), *Tfam* (*R*), and *Cycs* (*S*), and ATP levels (*T*) in WT and Sirt1cKO mice treated with DOI are expressed as fold change of WT+Veh ± SEM (*n* = 8–12 animals per group). *$P < 0.05$ (compared with WT, two-way ANOVA, Tukey's post hoc test).

that 5-HT also modulates mitochondrial mass and function in vivo. We next sought to modulate 5-HT levels in vivo, via activation of Pet1-positive serotonergic neurons (*SI Appendix*, Fig. S5 *L* and *M*) expressing the hM3Dq designer receptors exclusively activated by designer drugs (DREADD) coupled to Gq signaling in a bigenic hM3Dq/Pet1–Cre mouse line. hM3Dq/Pet1–Cre mice received the DREADD agonist clozapine-*N*-oxide (CNO) (3 mg/kg), which resulted in enhanced expression of c-Fos, a marker of neuronal activation within serotonergic neurons (*SI Appendix*, Fig. S5 *N* and *O*). We then determined the influence of chemogenetic activation of Pet1–Cre-positive serotonergic neurons (CNO; 3 mg/kg, once daily for 10 d) (Fig. 5*K* and *SI Appendix*, Fig. S1*P*) on mitochondrial biogenesis and function in the prefrontal cortex (PFC), which was selected due to the abundant expression of 5-HT$_{2A}$ receptors in this neocortical region. We observed a significant increase in mtDNA (Fig. 5*L*) and cellular ATP (Fig. 5*M*) levels in CNO-treated hM3Dq/Pet1–Cre mice compared with vehicle-treated controls. Western blot analysis revealed significant increases in SIRT1 (Fig. 5*N* and *SI Appendix*, Fig. S5*Q*), VDAC (Fig. 5*N* and *SI Appendix*, Fig. S5*R*), ATP5A (Fig. 5*N* and *SI Appendix*, Fig. S5*S*), and TFAM (Fig. 5*N* and *SI Appendix*, Fig. S5*T*) and a trend (*P* = 0.09) toward an increase for Cyt C (Fig. 5*N* and *SI Appendix*, Fig. S5*U*) protein

expression in the CNO-treated hM3Dq/Pet1–Cre group. Collectively, these results indicate that both 5-HT infusion into the cortex in a rat model and chemogenetic activation of serotonergic neurons in a mouse model can evoke changes in mitochondrial biogenesis and function in vivo.

We then addressed the contribution of SIRT1 to the effects of 5-HT$_{2A}$ receptor stimulation on mtDNA, gene expression of mitochondrial regulators, and ATP levels in vivo using conditional, cortical SIRT1 knockout (Sirt1cKO: Emx1–Cre; Sirt1$^{-/-}$) mice (Fig. 5*O*). While subchronic DOI administration resulted in a significant induction of mtDNA levels in WT animals, this was lost in Sirt1cKO mice (Fig. 5*P*). Furthermore, DOI treatment evoked an up-regulation of *Ppargc1a*, *Tfam*, and *Cycs*, in WT, but not in Sirt1cKO, mice (Fig. 5 *Q*–*S*). Furthermore, the DOI-mediated increase in cellular ATP levels was completely abrogated in Sirt1cKO mice (Fig. 5*T*). Collectively, these results establish that 5-HT$_{2A}$ receptor stimulation induces mitochondrial biogenesis and function through transcriptional control exerted by SIRT1.

Discussion

Our findings demonstrate that 5-HT regulates both mitochondrial biogenesis and function in cortical neurons, via the 5-HT$_{2A}$

receptor. Stimulation of the 5-HT$_{2A}$ receptor recruits the SIRT1–PGC-1α axis through PLC and MAPK signaling pathways, which enhance transcription of key factors such as NRF1 and TFAM that drive mitochondrial biogenesis. We show that SIRT1 is essential for the mitochondrial effects of 5-HT on cortical neurons. Furthermore, 5-HT enhances mitochondrial respiratory capacity, OXPHOS efficiency, and ATP production, an effect also recapitulated through 5-HT$_{2A}$ receptor stimulation. In agreement with our in vitro data, 5-HT$_{2A}$ receptor stimulation, direct 5-HT infusion into the neocortex, and chemogenetic activation of Pet1–Cre-immunopositive serotonergic neurons in hM3Dq/Pet1–Cre mice in vivo enhanced mitochondrial biogenesis, expression of several mitochondrial regulators, and ATP levels within the neocortex. The in vivo effects of 5-HT$_{2A}$ receptor stimulation on mitochondrial biogenesis and function were mediated via SIRT1. Our in vivo studies demonstrated increased state-2 and -3 respiration, indicative of enhanced mitochondrial capacity and OXPHOS efficiency, that contributed to an elevated ATP production rate in response to 5-HT$_{2A}$ receptor stimulation. Pre-exposure to 5-HT enhanced the ability of cortical neurons to buffer excitotoxic and oxidative stress, accompanied by a reduction in cellular ROS. SIRT1 was required for these prosurvival effects of 5-HT and 5-HT$_{2A}$ receptor stimulation, suggesting the intriguing possibility that the mitochondrial effects of 5-HT may underlie the enhanced stress adaptation noted in cortical neurons. Our findings indicate that 5-HT, through the 5-HT$_{2A}$ receptor, is an important upstream factor that regulates neuronal mitochondrial biogenesis and function via SIRT1 (Fig. 6). Furthermore, we highlight a robust prosurvival effect of 5-HT and DOI on cortical neurons when challenged with excitotoxic and oxidative insults, an effect mediated via SIRT1.

Prior reports indicated that specific 5-HT receptors can influence mitochondrial biogenesis in nonneuronal cells, such as renal proximal tubular cells and cardiomyocytes. In renal proximal tubular cells, 5-HT$_{1F}$ and 5-HT$_{2A}$ receptor activation promotes mitochondrial biogenesis through PGC-1α and enhances recovery following kidney injury (13, 14). In cardiomyocytes, 5-HT promotes cell survival via the 5-HT$_{2B}$ receptor and PI3K–

Akt and MAPK pathways (15). Perinatal selective serotonin reuptake inhibitor exposure is linked to increased mitochondrial respiratory capacity and reduced ROS levels in cardiac tissue (16) and liver (17), as well as sex-specific effects on brainstem mitochondrial function (18). Thus far, few studies have examined the direct influence of 5-HT on mitochondria in neurons. Mitochondrial transport in hippocampal neurons, is promoted by 5-HT via the 5-HT$_{1A}$ receptor (9). A recent study demonstrated that 5-HT$_{1F}$ receptor stimulation regulates mitochondrial biogenesis in nigral dopaminergic neurons and exerts neuroprotective effects in an animal model of Parkinson's disease (10). Our findings highlight a key role of 5-HT via the 5-HT$_{2A}$ receptor, PLC and MAPK pathways, and the SIRT1–PGC-1α axis in enhancing mitochondrial biogenesis and function both in cortical neurons in vitro and in the neocortex in vivo. While our results support a direct action of 5-HT/5-HT$_{2A}$ receptor stimulation on mitochondrial biogenesis and function in the neocortex, we cannot preclude the possibility of a role for indirect mechanisms exerted via peripheral actions of 5-HT. Collectively, these results highlight a putative prenervous trophic factor-like action of 5-HT on mitochondria and suggest the possibility that tissue-specific mitochondrial effects of 5-HT may involve distinct 5-HT receptors that facilitate cell survival and stress adaptation.

Interestingly, we did not observe any effect of NE and DA on mitochondrial biogenesis or ATP levels in cortical neurons. DA receptors have been linked to modulation of mitochondrial respiration in the nucleus accumbens (19) and to inhibition of mitochondrial motility in hippocampal neurons (20), suggesting that other monoamines could exert circuit-specific influences on mitochondria. In this vein, melatonin and N-acetylserotonin, a precursor for melatonin, both exhibit neuroprotective effects, hypothesized to involve inhibition of mitochondrial death pathways (21, 22). While these reports suggest that diverse monoamines could impinge on mitochondrial mechanisms as a component of their neuroprotective action, they do not address whether monoamines directly target neuronal mitochondrial biogenesis and bioenergetics and the underlying mechanisms. The focus of our studies
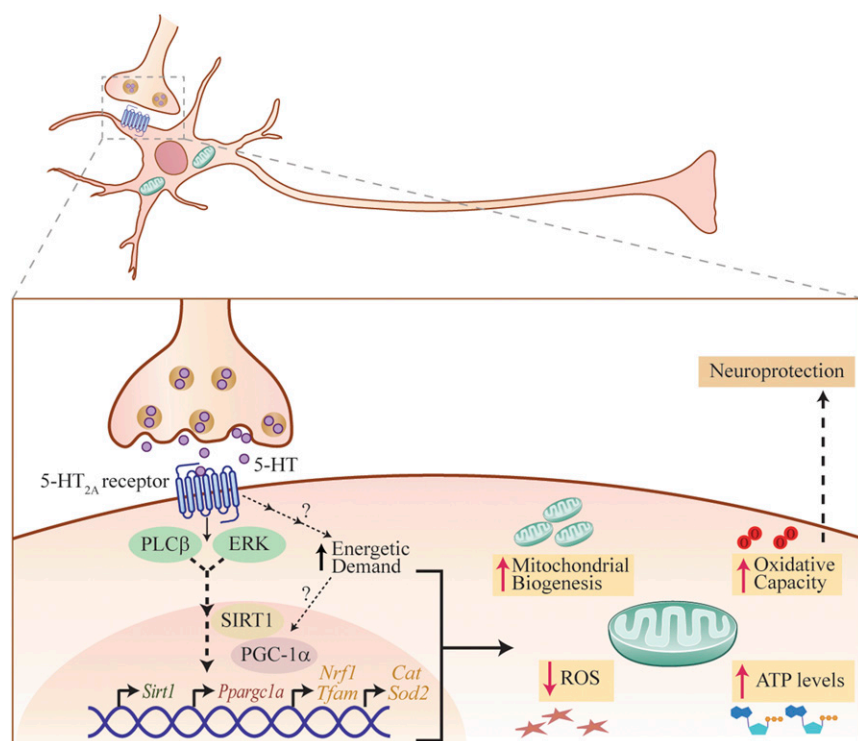
Fig. 6. Schematic depicting the putative mechanism for 5-HT effects on mitochondrial biogenesis and function. The model depicts 5-HT binding to the 5-HT$_{2A}$ receptor expressed by cortical neurons, which evokes an activation of the PLC and MAPK signaling pathways. This recruitment of PLC and MAPK signaling, likely through a multiple-step process, results in recruitment of SIRT1, which is a key regulator of mitochondrial biogenesis. SIRT1 may then modulate PGC-1α expression, which has been shown to be a master regulator of mitochondrial biogenesis and, in turn, could enhance NRF1 and mitochondrial transcription factor TFAM expression, thus mediating effects of 5-HT on mitochondrial biogenesis. Our results indicate that SIRT1 is required for the effects of both 5-HT and 5-HT$_{2A}$ receptor agonists on mitochondrial biogenesis. In addition, 5-HT and 5-HT$_{2A}$ receptor stimulation leads to an increase in basal OCR, which may reflect a heightened energetic demand that could, in turn, drive a transcriptional program, leading to a subsequent adaptive increase in mitochondrial content and function. Furthermore, 5-HT and 5-HT$_{2A}$ receptor agonists also enhance ATP production and increase OXPHOS, maximal respiration, and spare respiratory capacity. In addition, 5-HT also reduces cellular ROS levels and enhances expression of antioxidant enzymes in cortical neurons. This enhancement in mitochondrial biogenesis and function may contribute to the effects of 5-HT and 5-HT$_{2A}$ receptor agonists in conferring neuronal protection from excitotoxic and oxidative stress.

has been to address the impact of 5-HT on mitochondrial biogenesis and function; however, it is important to highlight that mitochondria are highly dynamic organelles that constantly undergo fission and fusion. We have not assessed effects of 5-HT on mitochondrial morphology and dynamics, which merit future investigation. Our in vivo studies were performed in adult animals, indicating that the mitochondrial effects of 5-HT are reflective of actions in the mature nervous system. Our results motivate future studies to assess the mitochondrial effects of 5-HT during developmental time windows.

The dose-dependent effects of 5-HT on mitochondrial biogenesis and bioenergetics were observed in the micromolar concentration range. The neurotransmitter 5-HT has both synaptic and extrasynaptic effects, and while synaptic vesicular concentrations are estimated as high as 6 mM, 5-HT can diffuse >20 μm away to extrasynaptic sites, where concentrations fall into the micromolar and nanomolar range (23, 24). The doses of 5-HT used in our study fall within this physiologically relevant range (23, 25–27). Furthermore, DREADD-mediated chemogenetic activation of Pet1-positive serotonergic neurons in vivo also resulted in enhanced mitochondrial mass and function. Pharmacological and genetic loss-of-function studies clearly demonstrate that the effects of 5-HT on mtDNA content, *Ppargc1a* and *Sirt1* expression, and ATP levels are mediated via the 5-HT$_{2A}$ receptor. Strikingly, while these effects of 5-HT are completely blocked by both pharmacological blockade or genetic loss of the 5-HT$_{2A}$ receptor, we did not observe a basal change in these measures. The absence of baseline mitochondrial changes suggests functional redundancy in the pathways that modulate neuronal mitochondrial biogenesis and function. The effects of 5-HT on mtDNA, gene expression, ATP levels, and OXPHOS were phenocopied by 5-HT$_{2A}$ receptor stimulation of cortical neurons and involved the PLC and MAPK, but not the PI3K–Akt, signaling pathways (Fig. 6). However, we do not preclude a role for additional signaling pathways that could be activated by the 5-HT$_{2A}$ receptor, as we restricted our analysis to only the major signaling cascades reported to lie downstream of 5-HT$_{2A}$ receptor stimulation (28).

It is noteworthy that both hallucinogenic (DOI) and non-hallucinogenic (Lisuride) ligands of the 5-HT$_{2A}$ receptor (29) can enhance mitochondrial biogenesis and ATP levels, suggesting a central role for the 5-HT$_{2A}$ receptor in neuronal bioenergetics. Prior reports indicated that 5-HT$_{2A}$ receptor stimulation enhances neurite outgrowth in cortical neurons (30) and is upstream of the regulation of trophic factors, such as BDNF (31). BDNF has been shown to enhance mitochondrial docking at synapses and regulate neuronal mitochondrial biogenesis via PGC-1α (32, 33). This motivates future experiments to examine the possibility of a coordinated interplay between 5-HT, the 5-HT$_{2A}$ receptor, and BDNF in regulation of trophic and neuroprotective effects, driven via an influence on mitochondria.

The influence of 5-HT on mitochondria in cortical neurons is exerted by a transcriptional cascade involving master regulators of mitochondrial biogenesis (SIRT1 and PGC-1α), whose expression is rapidly induced by 2–6 h, both in vitro and in vivo. This is followed by a return to baseline and a second phase of transcriptional activation at 48 h after sustained 5-HT/5-HT$_{2A}$ receptor stimulation, which precedes the effects on enhanced mitochondrial mass and function. This demonstrates that 5-HT exerts transcriptional control of the SIRT1–PGC-1α axis and indicates that priming of this axis may serve as the driver of the mitochondrial effects of 5-HT. Furthermore, pharmacological and genetic studies indicated that the effects of 5-HT on *Sirt1* and *Ppargc1a* expression are mediated through the 5-HT$_{2A}$ receptor. In this context, it is relevant to consider the possibility that the initiation of this transcriptional program by 5-HT/5-HT$_{2A}$ receptor stimulation could arise due to a heightened energetic demand, reflected by increased basal mitochondrial respiration,

serving as the precursor event that contributes to a subsequent adaptive increase in mitochondrial content and function (Fig. 6).

The SIRT1–PGC-1α axis activates a coordinated transcriptional program to meet cellular energy demands, via modulation of mitochondrial biogenesis and functions (6, 7). SIRT1-mediated deacetylation activates PGC-1α, a master regulator of expression of mitochondrial genes via NRF1 and TFAM (6, 8). NRF1 enhances expression of OXPHOS machinery and promotes TFAM expression, which drives transcription and replication of mtDNA (6, 7). Our results underscore the importance of SIRT1 for the effects of 5-HT and DOI on mitochondrial biogenesis and ATP levels. Pharmacological blockade or genetic ablation of SIRT1 in cortical neurons abrogated the effects of 5-HT on mitochondrial mass and cellular ATP levels. Furthermore, our in vivo studies indicated that the effects of DOI on gene expression, mitochondrial content, and ATP levels in the neocortex were absent in Sirt1cKO mice. However, SIRT1 perturbations did not result in any baseline changes, consistent with previous reports on SIRT1 loss of function and mitochondrial output (34, 35). This suggests that baseline regulation of mitochondrial biogenesis is likely modulated by multiple pathways. Interestingly, studies with genetic loss of PGC-1α are also similarly suggestive of functional redundancy, given they do not show major baseline defects in mitochondrial biogenesis and function (36). While our results do not allow us to conclude whether PGC-1α is essential for the effects of 5-HT/5-HT$_{2A}$ receptor stimulation, given that both SIRT1 and PGC-1α are established regulators of mitochondrial biogenesis/function (6, 8), our findings suggest that the 5-HT–mediated SIRT1-dependent mitochondrial effects likely involve a role for PGC-1α. Together, our results clearly illustrate that 5-HT or 5-HT$_{2A}$ receptor stimulation-dependent induction of mitochondrial biogenesis and functions requires SIRT1 in the cortical neurons.

In the context of neurons, the upstream factors that integrate environmental cues and then impinge on the SIRT1–PGC-1α axis to initiate mitochondrial biogenesis and facilitate adaptation in response to altered energetic demands remain elusive. Our findings demonstrate a hitherto-unidentified relationship between 5-HT and SIRT1, providing evidence that 5-HT is an upstream regulator of SIRT1. A previous study indicated that SIRT1 can modulate serotonergic neurotransmission via transcriptional effects on monoamine oxidase A expression (37), and our findings raise the tantalizing possibility of a reciprocal relationship between 5-HT and SIRT1 in the brain. Given the role of 5-HT in facilitating stress adaptation, this suggests the possibility that 5-HT could serve as a vital intermediary in enhancing stress adaptation of neurons through recruitment of the SIRT1–PGC-1α axis to enhance mitochondrial biogenesis and function, thus endowing neurons with enhanced capacity to buffer stress.

Strikingly, 5-HT resulted in a robust reduction in cellular ROS levels and significantly attenuated the enhanced ROS in cortical neurons subjected to excitotoxic and oxidative stress. The concomitant increases evoked by 5-HT in the ROS-scavenging enzymes *Sod2* and *Cat* suggest a role for these antioxidant enzymes in the effects of 5-HT on ROS. Furthermore, 5-HT/5-HT$_{2A}$ receptor stimulation enhanced cortical neuron viability across a wide range of doses for kainate and H_2O_2, a neuroprotective effect that required SIRT1. Neurons face unique energetic demands, and the ability of mitochondria to effectively respond to alterations of environment and buffer the "allostatic" load of stress defines the trajectory for neuronal survival (38). In this context, the robust effects of 5-HT/5-HT$_{2A}$ receptor stimulation on spare respiratory capacity may contribute to the improved neuronal survival observed in neurons challenged with stress. Spare respiratory capacity, through the ability to increase mitochondrial respiration when challenged with enhanced energy demands, equips cells with the ability to buffer extreme stress and serves as a critical factor determining neuronal survival (39). These are significant findings, given the emerging link between mitochondrial dysfunction and

mood disorders, in particular a decline in ATP levels, increased oxidative stress, and cortical apoptotic cell loss (40). Specifically, our findings motivate future investigation to address the relationship between the mitochondrial and behavioral effects of 5-HT, both in the context of the pathogenesis and treatment of mood disorders. There remains a limited understanding of potential drug targets to induce mitochondrial biogenesis/function (41–43), and our work supports the notion that the 5-HT_{2A} receptor may serve as a putative drug target to regulate mitochondrial physiology.

In conclusion, our findings demonstrate that 5-HT can increase mitochondrial biogenesis and function in cortical neurons, via a 5-HT_{2A} receptor-dependent recruitment of the SIRT1–PGC-1α axis. Through the 5-HT_{2A} receptor, 5-HT exerts robust neuroprotective effects on cortical neurons buffering against neurotoxic insults. SIRT1 lies downstream of 5-HT, through the 5-HT_{2A} receptor in cortical neurons, and is essential for the effects of 5-HT on mitochondrial biogenesis, expression of regulators of mitochondrial biogenesis, ATP levels, and enhanced cell viability under stress. These mitochondrial effects of 5-HT bear significance, in relation to the influence of 5-HT, in promoting cell survival, neuronal plasticity, stress adaptation, and regulation of senescence/aging.

Materials and Methods

SI Appendix contains a detailed description of materials and methods.

To establish in vitro primary cortical cultures, cortices were dissected from E18.5 rat or mutant mouse embryos and were cultured as described in *SI Appendix, SI Materials and Methods*. For in vivo experiments, male Sprague–Dawley rats (5–6 mo), WT and Sirt1cKO mice (15 mo), bigenic hM3Dq/Pet1–Cre mice (15 mo), and C57BL/6NCrl/Cri mice (5–6 mo) were used. Intracortical infusion of 5-HT was carried out via delivery through osmotic minipumps (Alzet 2001) implanted surgically in Sprague–Dawley rats. Experimental procedures were performed in accordance with the guidelines of the Committee for Supervision and Care of Experimental Animals, Government of India, and were approved by the Tata Institute of Fundamental Research (TIFR) Institutional Animal Ethics Committee (CPCSEA-56/1999).

1. Turlejski K (1996) Evolutionary ancient roles of serotonin: Long-lasting regulation of activity and development. *Acta Neurobiol Exp (Warsz)* 56:619–636.
2. Azmitia EC (2007) Serotonin and brain: Evolution, neuroplasticity, and homeostasis. *Int Rev Neurobiol* 77:31–56.
3. Lesch KP, Waider J (2012) Serotonin in the modulation of neural plasticity and networks: Implications for neurodevelopmental disorders. *Neuron* 76:175–191.
4. Mattson MP, Gleichmann M, Cheng A (2008) Mitochondria in neuroplasticity and neurological disorders. *Neuron* 60:748–766.
5. Mattson MP, Moehl K, Ghena N, Schmaedick M, Cheng A (2018) Intermittent metabolic switching, neuroplasticity and brain health. *Nat Rev Neurosci* 19:63–80.
6. Hock MB, Kralli A (2009) Transcriptional control of mitochondrial biogenesis and function. *Annu Rev Physiol* 71:177–203.
7. Scarpulla RC, Vega RB, Kelly DP (2012) Transcriptional integration of mitochondrial biogenesis. *Trends Endocrinol Metab* 23:459–466.
8. Wareski P, et al. (2009) PGC-1alpha and PGC-1beta regulate mitochondrial density in neurons. *J Biol Chem* 284:21379–21385.
9. Chen S, Owens GC, Crossin KL, Edelman DB (2007) Serotonin stimulates mitochondrial transport in hippocampal neurons. *Mol Cell Neurosci* 36:472–483.
10. Scholpa NE, Lynn MK, Corum D, Boger HA, Schnellmann RG (2018) 5-HT_{1F} receptor-mediated mitochondrial biogenesis for the treatment of Parkinson's disease. *Br J Pharmacol* 175:348–358.
11. Brunet A, et al. (2004) Stress-dependent regulation of FOXO transcription factors by the SIRT1 deacetylase. *Science* 303:2011–2015.
12. St-Pierre J, et al. (2006) Suppression of reactive oxygen species and neurodegeneration by the PGC-1 transcriptional coactivators. *Cell* 127:397–408.
13. Harmon JL, et al. (2016) 5-HT2 receptor regulation of mitochondrial genes: Unexpected pharmacological effects of agonists and antagonists. *J Pharmacol Exp Ther* 357:1–9.
14. Gibbs WS, et al. (2018) 5-HT1F receptor regulates mitochondrial homeostasis and its loss potentiates acute kidney injury and impairs renal recovery. *Am J Physiol Renal Physiol* 315:F1119–F1128.
15. Nebigil CG, Etienne N, Messaddeq N, Maroteaux L (2003) Serotonin is a novel survival factor of cardiomyocytes: Mitochondria as a target of 5-HT2B receptor signaling. *FASEB J* 17:1373–1375.
16. Braz GRF, et al. (2016) Neonatal SSRI exposure improves mitochondrial function and antioxidant defense in rat heart. *Appl Physiol Nutr Metab* 41:362–369.
17. Simões-Alves AC, et al. (2018) Neonatal treatment with fluoxetine improves mitochondrial respiration and reduces oxidative stress in liver of adult rats. *J Cell Biochem* 119:6555–6565.
18. Silva TLA, et al. (2018) Serotonin transporter inhibition during neonatal period induces sex-dependent effects on mitochondrial bioenergetics in the rat brainstem. *Eur J Neurosci* 48:1620–1634.
19. van der Kooij MA, et al. (2018) Diazepam actions in the VTA enhance social dominance and mitochondrial function in the nucleus accumbens by activation of dopamine D1 receptors. *Mol Psychiatry* 23:569–578.
20. Chen S, Owens GC, Edelman DB (2008) Dopamine inhibits mitochondrial motility in hippocampal neurons. *PLoS One* 3:e2804.
21. Zhou H, et al. (2014) N-acetyl-serotonin offers neuroprotection through inhibiting mitochondrial death pathways and autophagic activation in experimental models of ischemic injury. *J Neurosci* 34:2967–2978.
22. Yang Y, et al. (2015) Melatonin prevents cell death and mitochondrial dysfunction via a SIRT1-dependent mechanism during ischemic-stroke in mice. *J Pineal Res* 58:61–70.
23. Daws LC, Toney GM (2007) High-speed chronoamperometry to study kinetics and mechanisms for serotonin clearance in vivo. *Electrochemical Methods for Neuroscience,*

Frontiers in Neuroengineering, eds Borland AC, Michael LM (CRC/Taylor & Francis, Boca Raton, FL), pp 63–81.
24. Bunin MA, Wightman RM (1998) Quantitative evaluation of 5-hydroxytryptamine (serotonin) neuronal release and uptake: An investigation of extrasynaptic transmission. *J Neurosci* 18:4854–4860.
25. Riccio O, et al. (2009) Excess of serotonin affects embryonic interneuron migration through activation of the serotonin receptor 6. *Mol Psychiatry* 14:280–290.
26. Lavdas AA, Blue ME, Lincoln J, Parnavelas JG (1997) Serotonin promotes the differentiation of glutamate neurons in organotypic slice cultures of the developing cerebral cortex. *J Neurosci* 17:7872–7880.
27. Kondoh M, Shiga T, Okado N (2004) Regulation of dendrite formation of Purkinje cells by serotonin through serotonin1A and serotonin2A receptors in culture. *Neurosci Res* 48:101–109.
28. Millan MJ, Marin P, Bockaert J, Mannoury la Cour C (2008) Signaling at G-protein-coupled serotonin receptors: Recent advances and future research directions. *Trends Pharmacol Sci* 29:454–464.
29. González-Maeso J, et al. (2007) Hallucinogens recruit specific cortical 5-HT(2A) receptor-mediated signaling pathways to affect behavior. *Neuron* 53:439–452.
30. Ly C, et al. (2018) Psychedelics promote structural and functional neural plasticity. *Cell Rep* 23:3170–3182.
31. Vaidya VA, Marek GJ, Aghajanian GK, Duman RS (1997) 5-HT2A receptor-mediated regulation of brain-derived neurotrophic factor mRNA in the hippocampus and the neocortex. *J Neurosci* 17:2785–2795.
32. Cheng A, et al. (2012) Involvement of PGC-1α in the formation and maintenance of neuronal dendritic spines. *Nat Commun* 3:1250.
33. Su B, Ji Y-S, Sun XL, Liu X-H, Chen Z-Y (2014) Brain-derived neurotrophic factor (BDNF)-induced mitochondrial motility arrest and presynaptic docking contribute to BDNF-enhanced synaptic transmission. *J Biol Chem* 289:1213–1226.
34. Price NL, et al. (2012) SIRT1 is required for AMPK activation and the beneficial effects of resveratrol on mitochondrial function. *Cell Metab* 15:675–690.
35. Philp A, et al. (2011) Sirtuin 1 (SIRT1) deacetylase activity is not required for mitochondrial biogenesis or peroxisome proliferator-activated receptor-gamma coactivator-1alpha (PGC-1alpha) deacetylation following endurance exercise. *J Biol Chem* 286:30561–30570.
36. Dorn GW, 2nd, Vega RB, Kelly DP (2015) Mitochondrial biogenesis and dynamics in the developing and diseased heart. *Genes Dev* 29:1981–1991.
37. Libert S, et al. (2011) SIRT1 activates MAO-A in the brain to mediate anxiety and exploratory drive. *Cell* 147:1459–1472.
38. Picard M, McEwen BS, Epel ES, Sandi C (2018) An energetic view of stress: Focus on mitochondria. *Front Neuroendocrinol* 49:72–85.
39. Nicholls DG (2008) Oxidative stress and energy crises in neuronal dysfunction. *Ann N Y Acad Sci* 1147:53–60.
40. Allen J, Romay-Tallon R, Brymer KJ, Caruncho HJ, Kalynchuk LE (2018) Mitochondria and mood: Mitochondrial dysfunction as a key player in the manifestation of depression. *Front Neurosci* 12:386.
41. Manji H, et al. (2012) Impaired mitochondrial function in psychiatric disorders. *Nat Rev Neurosci* 13:293–307.
42. Onyango IG, et al. (2010) Regulation of neuron mitochondrial biogenesis and relevance to brain health. *Biochim Biophys Acta* 1802:228–234.
43. Uittenbogaard M, Chiaramello A (2014) Mitochondrial biogenesis: A therapeutic target for neurodevelopmental disorders and neurodegenerative diseases. *Curr Pharm Des* 20:5574–5593.

NEUROSCIENCE